Journal of Statistical Physics, Vol. 123, No. 1, April 2006 (© 2006)
DOI: 10.1007/s10955-005-9000-z

Tricritical Directed Percolation

S. Lübeck[1]

Received July 5, 2005; accepted October 2, 2005
Published Online: April 5, 2006

We consider a modification of the contact process incorporating higher-order reaction terms. The original contact process exhibits a non-equilibrium phase transition belonging to the universality class of directed percolation. The incorporated higher-order reaction terms lead to a non-trivial phase diagram. In particular, a line of continuous phase transitions is separated by a tricritical point from a line of discontinuous phase transitions. The corresponding tricritical scaling behavior is analyzed in detail, i.e., we determine the critical exponents, various universal scaling functions as well as universal amplitude combinations.

KEY WORDS: phase transition, tricritical behavior, directed percolation
PACS numbers: 05.70.Ln, 05.50.+q, 05.65.+b

1. INTRODUCTION

The concept of universality is well established for equilibrium critical phenomena where a unifying framework exists. Compared to the equilibrium situation less is known in case of non-equilibrium phase transitions. In particular a classification scheme of the rich and often surprising variety of non-equilibrium phase transitions is still lacking. Nevertheless, it is expected that analogous to equilibrium each non-equilibrium universality class is characterized by a certain symmetry. In this work we focus on stochastic processes which exhibit irreversible phase transitions into absorbing and fluctuation free states (see[1–4] for recent reviews). In that case the universality determining symmetry is expressed in a corresponding path integral formulation[2,5] which is associated to the considered stochastic process. A well known example is the universality class of directed percolation (DP). According to its robustness and ubiquity (including critical phenomena in

[1]Theoretische Physik, Universität Duisburg-Essen, 47048 Duisburg, Germany; e-mail: sven@thp.uni-duisburg.de

0022-4715/06/0400-0193/0 © 2006 Springer Science+Business Media, Inc.

physics, biology, as well as catalytic chemical reactions) directed percolation is recognized as the paradigm of non-equilibrium phase transitions into absorbing states. All non-equilibrium critical systems belong to the DP universality class if the associated absorbing phase transition is described by a single component order parameter and if the corresponding coarse grained system obeys the so-called rapidity reversal symmetry (at least asymptotically). Unfortunately, this symmetry is usally reflected on a coarse grained level only. Often, it is masked on a microscopic level, e.g. it is not reflected in the dynamic rules of certain lattice models. But the robustness of the DP universality class is expressed by the conjecture of Janssen and Grassberger[6,7]: short-range interacting systems, exhibiting a continuous phase transition into an absorbing state, belong to the DP universality class, if they are characterized by a one-component order parameter and no additional symmetries and no quenched disorder. This robustness of the DP universality class was recently demonstrated for five lattice models.[8] Despite the different interaction details (such as different lattice structures, different update schemes, different implementation schemes of the conjugated field, infinite and finite numbers of absorbing states, models with and without multiple particle occupation, etc.) all considered models are characterized by the same universal scaling functions. Different universality classes than DP occur if the rapidity reversal is broken, e.g. by quenched disorder,[9–14] or additional symmetries such as particle-hole symmetry (compact directed percolation[15,16]), particle conservation (Manna universality class[17–19]), or parity conservation (for example branching annihilating random walks with an even number of offsprings[20,21]).

Another universality class of absorbing phase transitions which is directly related to DP is tricritical directed percolation (TDP). Analogous to the ϕ^6-theory in equilibrium critical phenomena the process of TDP incorporates higher-order reaction terms than ordinary DP. Investigations of TDP in one-dimensional systems traces back to the seminal work of Grassberger.[7] Later, a field theoretical analysis was performed by Ohtsuki and Keyes[22,23] (see also[5,24]). In that work the authors discuss a one-component reaction-diffusion system that exhibits a tricritical point. This tricritical point separates continuous DP-like transitions from first-order transitions. Using an ϵ-expansion several critical exponents were estimated. Furthermore, the authors determine the upper critical dimension $D_c = 3$. Compared to the established field theory of TDP less work was done numerically. Several modifications of one-dimensional DP-lattice models are known which yield multicritical behavior. But mostly a bicritical point is observed or the occurring tricriticality is analyzed within a mean field level only (see e.g.[25–27]). Surprisingly no systematic numerical investigations of tricritical-DP scaling behavior were performed so far.

In this work we analyze the tricritical contact process (TCP). This model is a modification of the well-known contact process[28] which belongs to the universality class of directed percolation. The modification incorporates higher-order

particle reactions, in particular a pair reaction scheme is added. It is worth mentioning that multicritical behavior does not necessarily appear by introducing additional higher-order reaction schemes. Multicritical behavior occurs if the resulting lower-order reactions vanish on a coarse grained scale (see[23] and references therein). In our case, the added pair reaction scheme leads to a non-trivial phase diagram containing first- and second-order transitions as well as a tricritical point. In $D \geq 2$ the tricritical point separates a line of DP-like transitions from a line of first-order transitions. In one-dimension, preliminary results do indicate that the TCP does not exhibit a tricritical behavior. According to numerical simulations and to a mean field cluster analysis[29] the first-order line and the tricritical point collapse for $D = 1$ to the end point of the corresponding phase diagram (this agrees with the more general argument that first-order transitions can not occur in fluctuating one-dimensional systems due to the fact that the surface tension of a given domain does not depend on its size). Therefore, we focus on the higher-dimensional systems in the following. First, we survey the mean field behavior of TDP and of the TCP which are valid for $D > 3$. Second, the two-dimensional TCP is numerically examined. A scaling analysis of the DP-like transitions and of the tricritical phase transition itself is presented. In particular, the full crossover between both universality classes is recovered. The obtained values of universal quantities, such as the critical exponents, are compared to the results of the corresponding field theories.[5,22,23]

Furthermore, the regime of first-order transitions is investigated. Discontinuous phase transitions are of their own interest (see for example[27,30–32]) because most absorbing phase transitions are of second-order. As well known, discontinuous transitions are usually characterized by hysteresis cycles caused by the coexistence of two phases. A small but finite hysteresis can be observed in numerical simulations of the TCP.

2. TRICRITICAL DIRECTED PERCOLATION

The process of directed percolation might be represented by the Langevin equation (see e.g.[6])

$$\lambda^{-1}\partial_t \rho_a = \tau\rho_a - g\rho_a^2 - c\rho_a^3 + \Gamma\nabla^2\rho_a + h + \eta \; . \tag{1}$$

The particle density on a mesoscopic (coarse grained) scale $\rho_a = \rho_a(x, t)$ corresponds to the order parameter of the non-equilibrium phase transition. The control parameter of the transition τ describes the distance from the critical point $\tau = 0$. A finite positive particle density occurs above the transition point ($\tau > 0$) whereas the absorbing vacuum state ($\rho_a = 0$) is approached below the transition point. The external field h is conjugated to the order parameter and is usually implemented as a spontaneous particle creation process (see e.g.[33]). Furthermore, $\eta = \eta(x, t)$ denotes the noise which accounts for fluctuations of the particle

density. The noise η is a Gaussian random variable with zero mean and whose correlator is given by[6]

$$\langle \eta(x,t)\eta(x',t')\rangle = \lambda^{-1}\kappa\ \rho_{\mathrm{a}}(x,t)\delta(x-x')\delta(t-t')\ . \tag{2}$$

Notice, that the noise ensures that the systems is trapped in the absorbing state $\rho_{\mathrm{a}}(x,t)=0$. Furthermore, higher-order terms such as $\rho_{\mathrm{a}}(x,t)^3$, $\rho_{\mathrm{a}}(x,t)^4$, ... or $\nabla^4\rho_{\mathrm{a}}(x,t)$, $\nabla^6\rho_{\mathrm{a}}(x,t)$, ... are usually neglected because they are irrelevant under renormalization group transformations as long as $g>0$. Negative values of g give rise to a first-order phase transition whereas $g=0$ is associated with a tricritical point.[22,23] In the latter cases the cubic term ρ_{a}^3 cannot be neglected.

In the following we present a simple but instructive mean field treatment. Neglecting the noise term as well as spatial variations of the order parameter the steady state behavior ($\partial_t\rho_{\mathrm{a}}=0$) at zero field is given by

$$\rho_{\mathrm{a}}=0 \quad \vee \quad \rho_{\mathrm{a}}=-\frac{g}{2c}\pm\sqrt{\frac{\tau}{c}+\left(\frac{g}{2c}\right)^2}\ . \tag{3}$$

The first solution corresponds to the absorbing phase. According to a linear stability analysis it is stable for $\tau<0$ and unstable for ($\tau>0$). The solution with the $-$sign yields unphysical and unstable results. The $+$sign solution describes the order parameter as a function of the control parameter τ and of the additional scaling field g. For $g<0$, this solution is stable if $\tau>-g^2/4c$, otherwise it is unstable. Assuming that the system is in the active phase ($\rho_{\mathrm{a}}>0$) the order parameter jumps at the borderline ($\tau=-g^2/4c$) from $\rho_{\mathrm{a}}=|g|/2c$ to zero. Thus the absorbing and the active phase coexist between the spinodal $\tau=-g^2/4c$ and the line $\tau=0$ for $g<0$.

The tricritical behavior is obtained for $g=0$. The order parameter behaves for $\tau>0$ as

$$\rho_{\mathrm{a}}=(\tau/c)^{\beta_t} \tag{4}$$

with the tricritical order parameter exponent $\beta_{\mathrm{t}}=1/2$. For $g>0$, the active phase is stable for $\tau>0$ and unstable otherwise. Close to the transition points ($\tau=0$) the order parameter exhibits a directed percolation like behavior

$$\rho_{\mathrm{a}}=-\frac{g}{2c}+\sqrt{\frac{\tau}{c}+\left(\frac{g}{2c}\right)^2}\Big|_{\tau\ll\frac{g^2}{4c}}=\left(\frac{\tau}{g}\right)^{\beta_{\mathrm{DP}}}+\mathcal{O}(\tau^2) \tag{5}$$

with the exponent $\beta_{\mathrm{DP}}=1$. The amplitude of this power-law diverges for $g\to 0$, signaling the crossover to the tricritical behavior.

Sufficiently away from the critical line $\tau=0$ we observe again the tricritical behavior

$$\rho_{\mathrm{a}}=-\frac{g}{2c}+\sqrt{\frac{\tau}{c}+\left(\frac{g}{2c}\right)^2}\Big|_{\tau\gg\frac{g^2}{4c}}=\sqrt{\frac{\tau}{c}}+\mathcal{O}(\tau^{-1}) \tag{6}$$

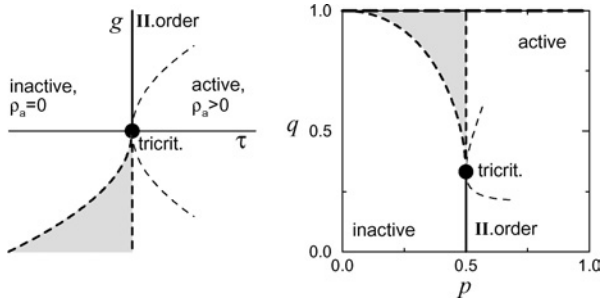

Fig. 1. The mean field phase diagrams of tricritical directed percolation (TDP). The left figure sketches the phase diagram as a function of the coarse grained variables τ and g (see Eq. (1)). The right figure shows the corresponding phase diagram as a function of the microscopic variables p and q, as defined by a reaction scheme of the tricritical contact process (see text). The thick lines correspond to second-order phase transitions (II.order) with $\beta_{\rm DP} = 1$. The bold circles mark the transition point of TDP with $\beta_{\rm t} = 1/2$. The shadowed areas indicate the coexistence of the absorbing and the active phase. The thin dashed lines illustrate the crossover to the tricritical behavior. In the right figure, two absorbing phases appear for $q = 1$ (long dashed lines). These phases are the fully occupied lattice (stable for $q > 0$) and the empty lattice (stable for $q < 1/2$).

for both $g > 0$ and $g < 0$. The crossover from the tricritical behavior takes place at

$$\tau = \mathcal{O}(g^2/4c) \; . \tag{7}$$

The complete phase diagram is sketched in Fig. 1.

Within the active phase for $g \geq 0$ the order parameter obeys the scaling form

$$\rho_{\rm a} = \lambda^{-\beta_{\rm t}} \tilde{r}_{\rm tDP}(\lambda\tau, g\lambda^{\phi}, h = 0) \tag{8}$$

for all positive λ and with the crossover exponent $\phi = 1/2$. In particular, $\lambda = g^{-1/\phi}$ leads to the scaling form

$$\frac{\rho_{\rm a}}{g^{\beta_{\rm t}/\phi}} = \tilde{r}_{\rm tDP}(\tau g^{-1/\phi}, 1, 0) \tag{9}$$

with

$$\tilde{r}_{\rm tDP}(x, 1, 0) \sim \begin{cases} x_{\rm DP}^{\beta} & \text{if } x \ll 1 \\ x^{\beta_{\rm t}} & \text{if } x \gg 1 \; . \end{cases} \tag{10}$$

In that way, the scaling plot $\rho_{\rm a}/g^{\beta_{\rm t}/\phi}$ vs. $\tau g^{-1}/\phi$ reflects the crossover from DP to TDP.

Now we consider the scaling behavior at non-zero conjugated field h. The tricritical order parameter behavior at criticality ($\tau = 0$ and $g = 0$) is given by

$$\rho_{\rm a} = (h/c)^{\beta_{\rm t}/\sigma_{\rm t}} \tag{11}$$

with the exponent $\sigma_t = 3/2$. At the tricritical point the equation of state obeys the scaling form

$$\rho_a = \lambda^{-\beta_t} \tilde{r}_{tDP}(\lambda\tau, g = 0, h\lambda^{\sigma_t}). \tag{12}$$

Instead of the above equation the so-called Widom-Griffiths scaling form

$$h = \lambda^{-\sigma_t} \tilde{h}_{tDP}(\lambda\tau, \rho_a\lambda^{\beta_t}, g = 0) \tag{13}$$

is often used to describe the scaling behavior of the equation of state. Despite metric factors the tricritical scaling form is given by

$$\tilde{h}_{tDP}(x, y, g = 0) = -xy + y^3. \tag{14}$$

The corresponding scaling form of ordinary DP $\tilde{h}_{DP}(x, y) = -xy + y^2$ reflects the different universality class.

For the sake of completeness we present the dynamical order parameter behavior at tricriticality

$$\begin{aligned} \rho_a(\tau = 0, g = 0, h = 0, t) \quad &= \quad \left(\rho_{a,t=0}^{-2} + 2ct\right)^{-1/2} \\ &\xrightarrow{t \to \infty} (2ct)^{-\alpha_t} \end{aligned} \tag{15}$$

with $\alpha_t = 1/2$. Furthermore, the steady state value of the order parameter (Eq. (4)) is approached from below as

$$\rho_a(\tau, g = 0, h = 0, t) = \sqrt{\frac{\tau}{c}}\left[1 - c_0 e^{-t/\xi_\parallel} + \mathcal{O}\left(e^{-2t/\xi_\parallel}\right)\right]. \tag{16}$$

Here, the constant c_0 contains the initial conditions and $\xi_\parallel$ denotes the temporal correlation length

$$\xi_\parallel = (2\tau)^{-\nu_{\parallel,t}} \tag{17}$$

with $\nu_{\parallel,t} = 1$. Incorporating spatial variations of the order parameter the spatial correlation length $\xi_\perp$ can be derived via an Ornstein-Zernicke approach. The resulting correlation length exponent $\nu_{\perp,t} = 1/2$ leads to the dynamical exponent $z_t = \nu_{\parallel,t}/\nu_{\perp,t} = 2$. Eventually we just mention that the tricritical exponent of the order parameter fluctuations is given by $\gamma'_{\perp,t} = 1/2$.[22] This value reflects a qualitative difference between the mean field scaling behavior of DP and TDP. In the latter case the fluctuations diverge at the transition point whereas they remain finite (jump) in case of DP.[34,35] Another difference between both universality classes concerns the value of the upper critical dimension, namely $D_c = 4$ for ordinary DP[36,37] and $D_c = 3$ for TDP.[22,23]

3. MODEL AND SIMULATIONS

We consider a modification of the contact process (CP). The CP was introduced by Harris in order to model the spreading of epidemics.[28] It is a continuous-time Markov process that is usually defined on a D-dimensional simple cubic lattice. A lattice site may be empty ($n = 0$) or occupied ($n = 1$) by a particle and the dynamics is characterized by spontaneously occurring processes, taking place with certain transition rates. In numerical simulations the asynchronous update is realized by a random sequential update scheme: A particle on a randomly selected lattice site i is annihilated with rate one, whereas particle creation takes places on an empty neighboring site with rate $\lambda N/2D$, i.e.,

$$n_i = 1 \quad \overrightarrow{1} \quad n_i = 0, \tag{18}$$

$$n_i = 0 \; \overrightarrow{\lambda N/2D} \; n_i = 1, \tag{19}$$

where N denotes the number of occupied neighbors of n_i. Note that the rates are defined as transition probabilities per time unit, i.e., they may be larger than one. Thus, rescaling the time will change the transition rates. In simulations a discrete time formulation of the contact process is performed. In that case a particle creation takes place at a randomly chosen neighbor site with probability $p = \lambda/(1 + \lambda)$ whereas particle annihilation occurs with probability $1 - p = 1/(1 + \lambda)$.

In the language of reaction-diffusion models the contact process is described by the reduced reaction scheme

$$A \longrightarrow 0, \quad A \longrightarrow 2A \tag{20}$$

which is controlled by the parameter p and where the quantity A represents a particle. According to Ohtsuki and Keyes[22,23] higher-order reactions may lead to a tricritical behavior as well as to a first-order behavior. Here, we additionally take into consideration the pair reaction

$$2A \longrightarrow 3A. \tag{21}$$

This reaction is controlled by a parameter q. Updating a given occupied lattice site i, we first perform the pair reaction scheme with probability q (otherwise a usual CP-update step is performed). If a randomly selected neighbor of i is occupied we add a third particle at an empty (also randomly selected) neighbor of the pair. If the lattice site i is isolated a usual update procedure of the CP is performed. The detailed reaction scheme is listed in Table I.

It is essential for the following that within our implementation the annihilation processes

$$A \longrightarrow 0, \quad AA \longrightarrow 0A, \quad AA \rightarrow A0 \tag{22}$$

take place with probabilities proportional to $(1 - q)$. Thus these reactions are suppressed for $q \approx 1$ and are eventually forbidden for $q = 1$. In that case particle

Table I. The reaction schemes and the corresponding probabilities of the considered tricritical contact process

Reaction	Probability
$A \longrightarrow 0$	$(1-q)(1-p)$
$0A \longrightarrow 00$	$q(1-p)$
$0A \longrightarrow AA$	$(1-q)p$
$AA \longrightarrow 0A$	$(1-q)(1-p)$
$0AA \longrightarrow \mathrm{AAA}$	q

Note. For $q = 0$ the reaction scheme of the original contact process is recovered (see text).

annihilation occur via the reactions

$$A0 \longrightarrow 00, \quad 0A \longrightarrow 00. \tag{23}$$

This implies that annihilation processes are restricted to the domain boundaries and do not occur insight of a domain. This behavior is reminiscent of compact directed percolation[15,16,38] where the density of particles exhibits a discontinuous behavior at the critical point.

The above scenario is also reflected by a corresponding mean field analysis. Within the simplest mean field approach (single site approximation), the order parameter is given by

$$\partial_t \rho_\mathrm{a} = \tau_{p,q}\rho_\mathrm{a} - g_{p,q}\rho_\mathrm{a}^2 - c_{p,q}\rho_\mathrm{a}^3 \tag{24}$$

with

$$\tau_{p,q} = 2p - 1, \quad g_{p,q} = p - (2-p)q, \quad c_{p,q} = q. \tag{25}$$

The tricritical point ($p_\mathrm{t} = 1/2, q_\mathrm{t} = 1/3$) is determined by the conditions $\tau = 0$ and $g = 0$. The line of second-order phase transitions ($p_\mathrm{c} = 1/2$ and $q < 1/3$) is obtained from $\tau = 0$ and $g > 0$. Within the first-order regime ($g < 0$) the absorbing phase is stable for $p < 1/2$. The borderline of stability of the active phase ($p_\mathrm{a} > 0$) is determined by $\tau = -g^2/4c$. The corresponding mean field phase diagram is sketched in Fig. 1.

For $q = 1$ the corresponding mean field differential equation is given by

$$\partial_t \rho_\mathrm{a} = (2p-1)\rho_\mathrm{a}(1-\rho_\mathrm{a}) + \rho_\mathrm{a}^2(1-\rho_\mathrm{a}). \tag{26}$$

Obviously, the steady state solutions are the empty lattice ($\rho_\mathrm{a} = 0$ stable for $p < 1/2$) and the fully occupied lattice ($\rho_\mathrm{a} = 1$ stable for $p > 0$). Note that both phases coexist for $p < 1/2$. It is worth to compare the TCP for $q = 1$ to the process of compact directed percolation which is described by the equation (see e.g.[5])

$$\partial_t \rho_\mathrm{a} = (2p-1)\rho_\mathrm{a}(1-\rho_\mathrm{a}). \tag{27}$$

Here, the fully occupied lattice is stable for $p > 1/2$ whereas the empty lattice is stable for $p < 1/2$. Thus the process of compact directed percolation displays no phase coexistence in contrast to the tricritical contact process for $q = 1$. Furthermore, Eq. (27) clearly express the particle-hole symmetry which is the characteristic symmetry of the universality class of compact directed percolation. In case of the TCP for $q = 1$, the particle-hole symmetry is broken by the pair reaction processes contributing $\rho_a^2(1 - \rho_a)$ to the equation of motion.

Analyzing numerically or experimentally the scaling behavior of tricritical systems it is crucial to determine the value of the tricritical point with high accuracy. Thus a sensitive criterion is required to distinguish a first-order transition from a second-order transition. At first glance, one is tempted to make use of the order parameter jump at the first-order transition. At the tricritical point the order parameter changes its behavior from a discontinuous jump to a continuous power-law. But first, this behavior is affected close to the tricritical point by crossover effects (see Fig. 1). Second, it is notoriously difficult to distinguish a continuous phase transition with a small but finite value of the exponent β_t from a discontinuous jump. Especially this situation occurs in case of two-dimensional TDP. An alternative way is to investigate instead of the order parameter the order parameter fluctuations which diverge at the tricritical point but remain finite within the first-order regime. But the fluctuation measurements suffer by crossover effects in a similar way as the order parameter, i.e., a corresponding analysis yields therefore no significant improvement.

In order to circumvent these problems we apply a method of analyzing that is based on the scaling behavior of the order parameter close to the tricritical point within the second-order transition regime. In particular, the scaling form of the order parameter is used to recover the complete crossover from ordinary DP to the TDP. We assume that the order parameter as well as the order parameter fluctuations obey the scaling forms

$$\rho_a \sim \lambda^{-\beta_t} \tilde{r}_{tDP}(\lambda\tau, g\lambda^{\phi}, h = 0) \tag{28}$$

$$\Delta\rho_a \sim \lambda^{\gamma_t'} \tilde{d}_{tDP}(\lambda\tau, g\lambda^{\phi}, h = 0) \tag{29}$$

with the so far unknown tricritical exponents β_t, γ_t', and ϕ. Asymptotically, the scaling functions have to fulfill the power-laws

$$\tilde{r}_{tDP}(x, 1, 0) \sim \begin{cases} x^{\beta_{DP}} & \text{if } x \ll 1 \\ x^{\beta_t} & \text{if } x \gg 1 \end{cases} \tag{30}$$

$$\tilde{d}_{tDP}(x, 1, 0) \sim \begin{cases} x^{-\gamma_{DP}'} & \text{if } x \ll 1 \\ x^{-\gamma_t'} & \text{if } x \gg 1 \end{cases} \tag{31}$$

The values of the exponents β_{DP} and γ_{DP}' are known with sufficient accuracy (see Table II and references therein). A serious problem is caused by the fact that the scaling forms contain the coarse grained variables τ and g. In general, these

Table II. The critical exponents and various universal amplitude combinations of tricritical (TDP) and ordinary directed percolation (DP) for various dimensions *D*

	$\mathrm{TDP}_{D=2}$	$\mathrm{TDP}_{D>3}$	$\mathrm{DP}_{D=2}$ [35,43,46,47]	$D=3$ [35,43,48]	$\mathrm{DP}_{D>4}$
β	0.14 ± 0.02	1/2	0.5834 ± 0.0030	0.813 ± 0.009	1
$\nu_\perp$	0.59 ± 0.08	1/2	0.7333 ± 0.0075	0.584 ± 0.005	1/2
$\nu_\parallel$	1		1.2950 ± 0.0060	1.110 ± 0.010	1
σ	1.12 ± 0.05	3/2	2.1782 ± 0.0171	2.049 ± 0.026	2
γ'	0.93 ± 0.06	1/2	0.2998 ± 0.0162	0.126 ± 0.023	0
γ	1.00 ± 0.06	1	1.5948 ± 0.0184	1.237 ± 0.023	1
$\eta_\perp$	0.42 ± 0.24	1	1.5912 ± 0.0148	1.783 ± 0.016	2
D_f	1.76 ± 0.05	2	1.2044 ± 0.0091	1.608 ± 0.019	2
β'		1	$\beta = \beta'$	$\beta = \beta'$	1
δ		1	0.4505 ± 0.0010	0.732 ± 0.004	1
α		1/2	$\alpha = \delta$	$\alpha = \delta$	1
θ		0	0.2295 ± 0.0010	0.114 ± 0.004	0
z		2	1.7660 ± 0.0016	1.901 ± 0.005	2
$\frac{X(+1,0)}{X(-1,0)}$	0.35 ± 0.05	1/2	0.25 ± 0.01	0.65 ± 0.03	1
U	0.84 ± 0.04		0.704 ± 0.013	0.61 ± 0.02	1/2

Note. The crossover exponent from tricritical to ordinary DP is given by $\phi_{D=2} = 0.55 \pm 0.03$ and $\phi_\mathrm{MF} = 1/2$.

variables depend on the (microscopic) parameters p and q in an unknown way. But there exists a certain window of scaling where the coarse grained variables can be replaced by the model parameters p and q. This will allow the determination of the tricritical point as well as of the exponents β_t and γ_t'.

In the following the system is investigated within the active phase close to the line of second-order phase transitions, i.e., $g(p,q) > 0$ and $\tau(p,q)$ close to zero. Performing simulations, the order parameter is measured as a function of p for fixed q. Sufficiently close to the transition line $p_\mathrm{c}(q)$ the coarse grained variable is approximated

$$\begin{aligned} \tau(p,q) &= \tau(p_\mathrm{c}(q) + \delta p, q) \\ &\approx \underbrace{\tau(p_\mathrm{c}(q),q)}_{=0} + \left.\frac{\partial \tau}{\partial p}\right|_{pc(q)} \delta p \end{aligned} \tag{32}$$

with $\delta p = p - p_\mathrm{c}(q)$. Since the derivative is taken at the transition line $p_\mathrm{c}(q)$ its value depends on the parameter q. But close to the tricritical point we yield up to higher-orders

$$\tau(p,q) \approx \left.\frac{\partial \tau}{\partial p}\right|_{p_c(q_t)} \delta p + \mathcal{O}(\delta p \delta q) \tag{33}$$

with $\delta q = q_t - q$.

A similar approximation can be obtained for $g(p, q)$. In the vicinity of the critical line we use the approximation

$$\begin{aligned} g(p, q) &= g(p_c(q) + \delta p, q) \\ &\approx g(p_c(q), q) + \frac{\partial g}{\partial p}\Big|_{p_c(q)} \delta p. \end{aligned} \tag{34}$$

Sufficiently close to the tricritical point we obtain

$$\begin{aligned} g(p, q) \approx \nabla g \cdot \underline{t}\Big|_{p_t, q_t} \delta q \\ + \frac{\partial g}{\partial p}\Big|_{p_t, q_t} \delta p + \mathcal{O}(\delta p \delta q), \end{aligned} \tag{35}$$

with $\nabla g = (\partial_p g, \partial_q g)$ and where the tangential vector along the phase boundary is denoted by $t = (\partial p_c(q)/\partial q, 1)$. Assuming that $\nabla g \cdot \underline{t}$ and $\partial g/\partial p$ are of the same order at the tricritical point, the coarse grained variable $g(p, q)$ can be replaced in the scaling functions Eqs. (30, 31) by the reduced model parameter δq if

$$\delta p \ll \delta q. \tag{36}$$

This condition Eq. (36) is fulfilled if the simulations are performed in a way that the distance to the phase boundary is smaller than the distance to the tricritical point. Thus, the order parameter and its fluctuations obey for $\delta_q > 0$ the scaling forms

$$\rho_a \sim \lambda^{-\beta_t} \tilde{r}_q(\lambda \delta p, \delta q \lambda^{\phi}, h = 0), \tag{37}$$

$$\Delta\rho_a \sim \lambda^{\gamma_t'} \tilde{d}_q(\lambda \delta p, \delta q \lambda^{\phi}, h = 0) \tag{38}$$

if the critical point $p_c(q)$ is approached along q = const paths (as indicated by the index q). The above scaling forms are not valid if $\nabla g \perp \underline{t}$ or if the derivative $\partial\tau/\partial p$ vanishes at the tricritical point. In the latter case higher-orders ($\mathcal{O}(\delta p^2)$) are required to describe the scaling behavior.

In the next section we describe the analysis of the simulation data. In particular, we have measured the averaged density of active sites $\rho_a(p, q, h) = \langle L^{-D} N_a \rangle$, i.e., the order parameter as a function of p and q and of the conjugated field h. Numerically obtained order parameter curves for $q = 0$ and for different values of the conjugated field are plotted in Fig. 2. The conjugated field is implemented via a generation of particles ($0 \longrightarrow A$ with probability h). It results in a rounding of the zero field curves and the order parameter behaves smoothly as a function of the control parameter for finite field values. For $h \longrightarrow 0$ we recover the non-analytical order parameter behavior. Additionally to the order parameter, we investigate the order parameter fluctuations $\Delta\rho_a(p, g, h) = L^D(\langle \rho_a^2 \rangle - \langle \rho_a \rangle^2)$ and the susceptibility $\chi(p, q, h) = \partial\rho_a/\partial h$. The susceptibility is obtained by performing

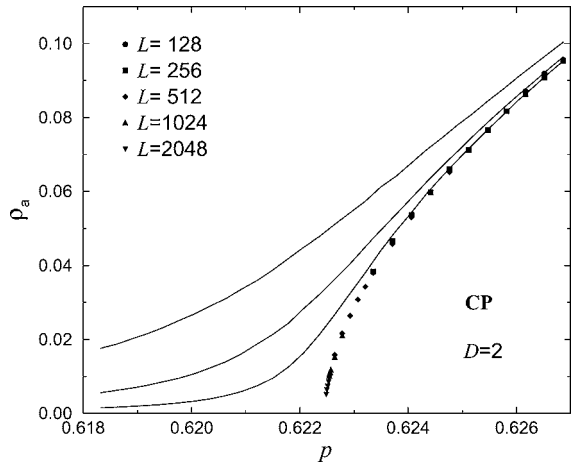

Fig. 2. The order parameter ρ_a of the two-dimensional contact process (CP) as a function of the control parameter p. The data are obtained from simulations on a simple cubic lattices of linear size L for various field values (from 10^{-6} to $h = 10^{-5}$). For non-zero field ρ_a exhibits an analytical behavior (lines). For zero field (symbols) the order parameter vanishes at the transition point $p = 0.62246^{(39)}$.

the numerical derivative of the order parameter ρ_a with respect to the conjugated field h.

4. SECOND-ORDER PHASE TRANSITION: DIRECTED PERCOLATION BEHAVIOR

According to the above analysis we have simulated the tricritical contact process (TCP) and have measured ρ_a as a function of p, keeping q fixed. Order parameter curves for various q-value are shown in Fig. 3. According to Eq. (37) these different curves collapse onto a single curve if the rescaled order parameter $\rho_a \delta q^{-\beta_t/\phi}$ is plotted as a function of the rescaled control parameter $\delta p \delta q^{-1/\phi}$. Therefore, we vary the parameters β_t, ϕ as well as q_t until a data collapse is obtained. Convincing results are obtained for $\beta_t = 0.14 \pm 0.02$, $\phi = 0.55 \pm 0.03$ and $q_t = 0.9055 \pm 0.0020$. A corresponding scaling plot is shown in Fig. 4. The data are obtained from simulations for 16 different values of q ranging from $q = 0.55$ up to $q = 0.904$. Typical distances to the critical line are of the order of $\mathcal{O}(\delta p) = 10^{-4}$. On the other hand the minimal distance δq to the tricritical point along the q-axis is larger than 0.0015. In, that way, the condition Eq. (36) is fulfilled, justifying the use of the scaling forms.

Since the entire crossover region covered several decades it could be difficult to observe small but systematic differences between the scaling functions of both models. It its therefore instructive to examine the crossover via the so-called

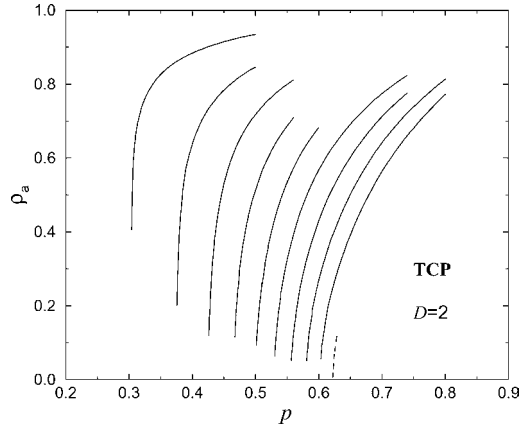

Fig. 3. The order parameter ρ_a of the tricritical contact process (TCP) as a function of the control parameter p for various values of $q \in \{0, 0.1, 0.2, 0.3, \ldots, 0.9\}$ (from right to left). The dashed line corresponds to the pure contact process ($q = 0$). The data are obtained from simulations on simple cubic lattices of linear size $L = 64, 128, \ldots, 512$.

effective exponent

$$\beta_{\text{eff}} = \frac{\partial}{\partial \ln x} \ln \tilde{r} q(x, 1, 0). \tag{39}$$

The corresponding data are shown in Fig. 5. The excellent data collapse of β_{eff} over more than 6 decades reflects the accuracy of the determination of the tricritical point.

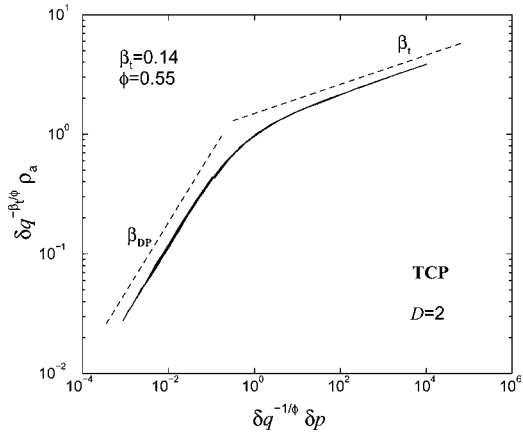

Fig. 4. The crossover scaling function of the order parameter at zero field. The dashed lines correspond to the asymptotic behaviors, i.e., to the ordinary DP and to the tricritical DP behavior (see Eq. (30)).

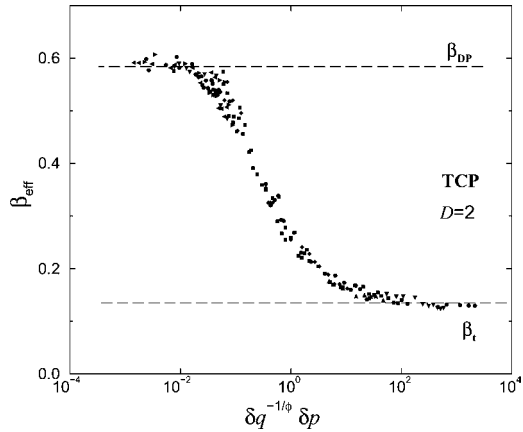

Fig. 5. The effective exponent $\beta_{\rm eff}$ of the order parameter. Both asymptotic scaling regimes (β_t and $\beta_{\rm DP}$) as well as the crossover regime are clearly recovered.

A similar crossover scaling analysis can be performed for the order parameter fluctuations. In that case, we use the above determined values of β_t, q_t and vary the value of the fluctuation exponent γ_t' until a data collapse of the different q-curves occurs. Figure 6 shows the corresponding data collapse as well as the effective exponent

$$\gamma'_{\rm eff} = \frac{\partial}{\partial \ln x} \ln \tilde{d}_q(x, 1, 0). \tag{40}$$

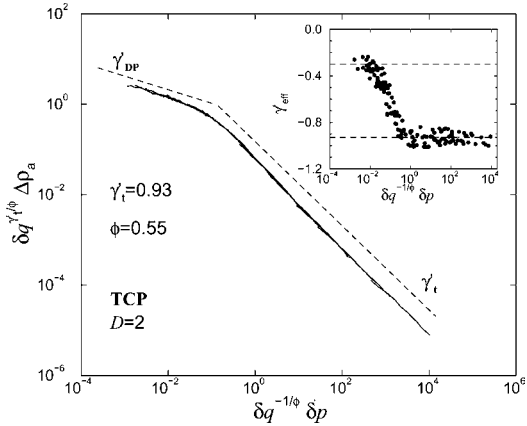

Fig. 6. The crossover scaling function of the order parameter fluctuations at zero field. The dashed lines correspond to the asymptotic behaviors, i.e., to the ordinary DP and to the tricritical DP behavior (see Eq. (31)). The inset displays the corresponding effective exponent $\gamma'_{\rm eff}$.

Although the data of the effective exponent are suffering from statistical fluctuations both asymptotic scaling regimes as well as the crossover regime can be identified. Worth mentioning, the crossover scaling function exhibits a so-called non-monotonic crossover.[40] Unfortunately, the statistical scattering of the effective exponent data masks the non-monotonic behavior from $\gamma_t' = 0.93 \pm 0.06$ to γ_{DP}'.

In summary, the crossover scaling analysis allows the determination of the tricritical value q_{t} with high accuracy. Furthermore, the effective exponents β_{eff} and γ_{eff}' reflect the full crossover from tricritical DP to ordinary DP which spans more than 6 decades.

5. SECOND-ORDER PHASE TRANSITION: TRICRITICAL BEHAVIOR

In the previous section we have determined the tricritical value q_t as well as the critical line $q(p_{\mathrm{c}})$ of the directed percolation like phase transitions. This yield a first glance of the phase diagram which is presented in Fig. 7. We now investigate the tricritical scaling behavior in detail. Therefore, we consider first the order parameter at zero field in the vicinity of the tricritical point. Second a conjugated field is applied which allows the determination of various universal quantities such as tricritical exponents, scaling functions as well as amplitude combinations.

In the following analysis, the tricritical point is approached in three different ways and the order parameter is determined at zero field (see Fig. 7). First, ρ_{a} is examined within the active phase as a function of p at the tricritical value

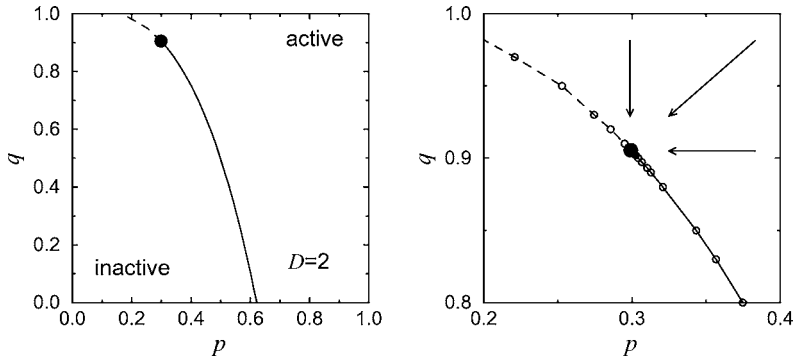

Fig. 7. The phase diagram of the two-dimensional modified contact process. The solid line marks continuous phase transitions which belong to the universality class of directed percolation. The dashed line corresponds to first-order phase transitions and the bold circle indicates the tricritical point. The small circles in the right figure show where the transitions points are determined numerically. Furthermore, the tricritical point is approached in the simulations along three different ways illustrated by the three arrows.

$q = 0.9055$. This yields the estimate

$$p_t = p_c(q_t = 0.9055) = 0.29931 \pm 0.00003. \tag{41}$$

Second, the order parameter is measured for $p = 0.29931$ as a function of q. From this analysis we obtain

$$q_c(p_t = 0.29931) = 0.90552 \pm 0.00005 \tag{42}$$

which agrees with the above determined value $q_t = 0.9055 \pm 0.0020$. To check these estimates the critical point is approached along a third path which is (more or less) perpendicular to the phase boundary. As well known the leading order of the scaling behavior, i.e., the critical exponents, do not depend on the way the critical point is approached. But the prefactors of the corresponding power-laws and the corrections to the leading scaling order are affected by the different directions. Thus the scaling behavior of the order parameter obeys asymptotically

$$\rho_{\mathrm{a}} \sim (a_p \delta p)^{\beta_t} \quad \text{for} \quad q = q_t \tag{43}$$

$$\rho_{\mathrm{a}} \sim (a_q \delta q)^{\beta_t} \quad \text{for} \quad p = p_t \tag{44}$$

$$\rho_{\mathrm{a}} \sim (a_\perp \delta p)^{\beta_t} \quad \text{along the perpendicular path.} \tag{45}$$

Plotting the corresponding data accordingly (e.g. ρ_{a} as a function of $(a_p \delta p)^{\beta_{\mathrm{t}}}$) the three different curves collapse asymptotically to the leading tricritical behavior if the so-called non-universal metric factors $a_p, a_q, a_\perp$ are chosen appropriately. The leading tricritical behavior corresponds in that analysis to a straight line with slope one. As can be clearly seen in Fig. 8 all three curves approach the tricritical scaling behavior asymptotically, confirming the accuracy of the determination of the tricritical point and of the order parameter exponent β_{t}. Furthermore, the corrections to scaling, i.e., the deviations to the asymptotical power-law depend strongly on the way the tricritical point is approached. Surprisingly, the smallest corrections occurs along the path p = const and not as usually expected along the way which is perpendicular to the phase boundary.

So far we have considered the order parameter at zero field in the vicinity of the tricritical point. Applying an external field which is conjugated to the order parameter, it is possible to investigate the scaling behavior of the tricritical equation of state. Again, the conjugated field is implemented via a generation of particles ($0 \longrightarrow A$ with probability h). Sufficiently close to the tricritical point ($g = 0$) the order parameter obeys the scaling form

$$\begin{aligned} \rho_{\mathrm{a}}(\tau_{p,q}, g_{p,q}, h) &\sim \lambda^{\beta_t} \tilde{r}(\lambda \tau_{p,q}, g\lambda^{\phi}, h\lambda^{\sigma_t})\Big|_{g=0} \\ &= \lambda^{-\beta_t} \tilde{r}(\lambda \tau_{p,q}, 0, h\lambda^{\sigma_t}). \end{aligned} \tag{46}$$

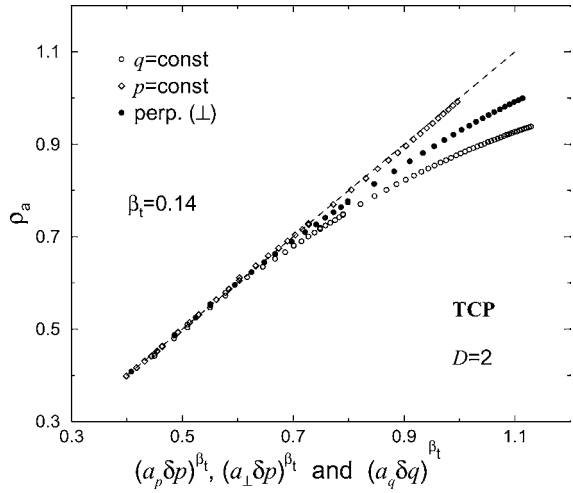

Fig. 8. The order parameter behavior of the tricritical contact process (TCP). The tricritical point is approached along three different ways indicated by the three different symbols. All three curves tend asymptotically to the function $f(x) = x$ (the dashed line corresponds to the pure tricritical power-law behavior) if ρ_a is plotted as a function of $(a_p \delta p)^{\beta_\mathrm{t}}$, $(a_q \delta q)^{\beta_\mathrm{t}}$, and $(a_\perp \delta p)^{\beta_\mathrm{t}}$, respectively. But as can be seen the corrections to scaling depend on the scaling direction.

Here, $\tau_{p,q}$ describes the distance to the tricritical point within the p–q–plane. All non-universal system dependent features (such as the lattice structure or the way the tricritical point is approached, etc.) can be absorbed in two metric factors a_path and a_h. Once the non-universal metric factors are chosen in a specific way, the scaling function $\tilde{R}$ (in contrast to $\tilde{r}$) is the same for all systems belonging to the universality class of directed percolation. Thus the universal scaling behavior is described by the ansatz

$$\rho_\mathrm{a}(\tau_{p,q}, 0, h) \sim \lambda^{-\beta_\mathrm{t}} \tilde{R}(\lambda a_\mathrm{path} \tau_\mathrm{path}, 0, a_h h \lambda^{\sigma_\mathrm{t}}) \tag{47}$$

yielding for $a_h h \lambda^{\sigma_\mathrm{t}} = 1$

$$\rho_\mathrm{a}(\tau_{p,q}, 0, h) \sim (a_h h)^{-\beta_\mathrm{t}/\sigma_\mathrm{t}} \tilde{R}(a_\mathrm{path} \tau_\mathrm{path} (a_h h)^{1/\sigma_\mathrm{t}}, 0, 1). \tag{48}$$

Throughout this work we use the conditions $\tilde{R}(1, 0, 0) = \tilde{R}(0, 0, 1) = 1$ to specify the metric factors which can be obtained from the amplitudes of the corresponding power-laws (see e.g. Eqs. (43)–(45)).

In order to determine the universal scaling form of the equation of state we have measured the field dependence of the order parameter. Again the tricritical point is crossed along three different paths in the p–q–plane. Along each path, ρ_a. is determined as a function of the distance to the tricritical point for at least

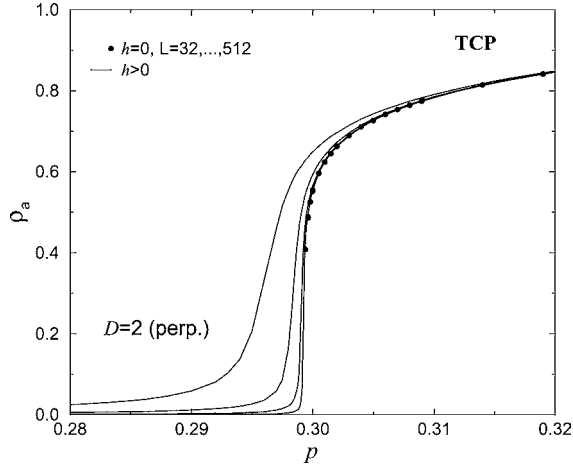

Fig. 9. The order parameter ρ_a of the two-dimensional tricritical contact process (TCP) close to the tricritical point. The tricritical point is crossed perpendicular to the phase boundary (see Fig. 1). The order parameter is plotted as a function of the control parameter r. The zero field data (circles) are obtained from simulations on a simple cubic lattices of linear size $L = 64, 128, 256, 512$. The solid curves correspond to the non-zero field behavior (from $h = 210^{-3}$ to $h = 310^{-5}$).

four different field values. The results are plotted for the perpendicular path in Fig. 9. According to the scaling form Eq. (48) the rescaled order parameter is plotted as a function of the rescaled distances to the tricritical point. In our analysis we have varied the field exponent σ_t until a data collapse is obtained. Convincing results are obtained for $\sigma_t = 1.20 \pm 0.05$ and are shown in Fig. 10. Since data of different scaling directions are considered the presented data collapse is an impressive demonstration of the universality class of TDP. Furthermore, the tricritical universal scaling function differs significantly from the corresponding scaling function of ordinary DP, reflecting the different universality classes.

Additionally to the order parameter behavior we have investigated the order parameter fluctuations $\Delta\rho_a$ as well as the order parameter susceptibility χ. The scaling behavior of both quantities is described by[8]

$$a_\Delta \Delta\rho_a(\tau_{p,q}, 0, h) \sim \lambda^{\gamma_t'} \tilde{D}(\lambda a_{\text{path}} \tau_{\text{path}}, 0, a_h h \lambda^{\sigma_t}), \tag{49}$$

$$a_\chi \chi(\tau_{p,q}, 0, h) \sim \lambda^{\gamma_t} \tilde{X}(\lambda a_{\text{path}} \tau_{\text{path}}, 0, a_h h \lambda^{\sigma_t}). \tag{50}$$

Setting $\tilde{D}(0, 0, 1) = 1$ the non-universal metric factor a_Δ is specified. Taking into account that the susceptibility is defined as the derivative of the order parameter with respect to the conjugated field we find $a_\chi = a_h^{-1}$,

$$\tilde{X}(x, 0, y) = \partial_y \tilde{R}(x, 0, y), \tag{51}$$

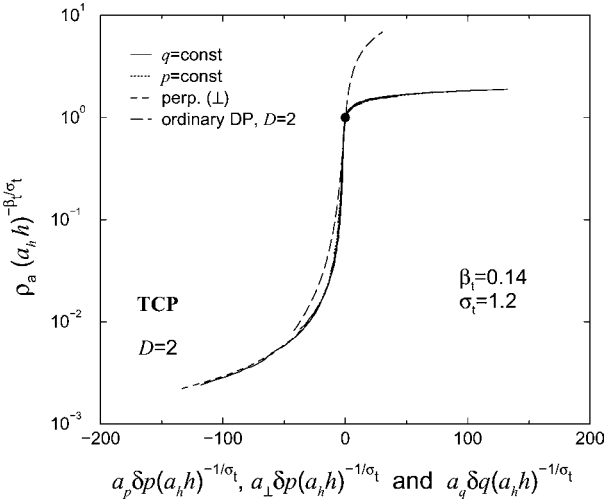

Fig. 10. The universal scaling function $\tilde{R}(x, 0, 1)$ of the universality class of TDP. For all three scaling directions (only the data within the scaling regime are plotted) at least four different curves are plotted corresponding to four different field values. The circle marks the condition $\tilde{R}(0, 0, 1) = 1$. The dashed line corresponds to the universal scaling function of ordinary DP (taken from[8]).

$$\tilde{\mathrm{X}}(0, 0, 1) = \frac{\beta_\mathrm{t}}{\sigma_\mathrm{t}}, \tag{52}$$

$$\gamma_\mathrm{t} = \sigma_\mathrm{t} - \beta_\mathrm{t}. \tag{53}$$

The latter equation corresponds to the Widom scaling law in equilibrium. Furthermore, Eq. (52) offers a useful consistency check of the numerical analysis.

The universal scaling functions of the order parameter fluctuations and the order parameter susceptibility are shown in Figs. 11 and 12, respectively. The susceptibility is obtained by performing the numerical derivative of the order parameter with respect to the conjugated field. Both scaling functions exhibit a maximum signaling the divergence of $\Delta\rho_a$ and χ at the tricritical point. The susceptibility data fulfill Eq. (52), reflecting the accuracy of the performed analysis. In both cases, the obtained universal scaling functions differ significantly from the corresponding scaling functions of ordinary DP.

Additionally to the critical exponents and universal scaling functions it is useful to investigate universal amplitude combinations. An often considered amplitude combination is related to the susceptibility behavior below and above the transition. For e.g. q = const the susceptibility diverges as

$$\chi(\delta p > 0, g = 0, h = 0) \sim a_{\chi,+}\delta p^{-\gamma_\mathrm{t}}, \tag{54}$$

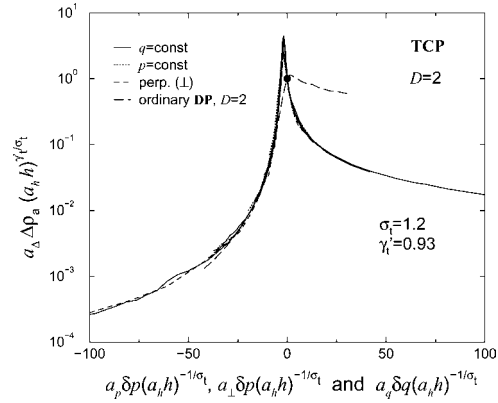

Fig. 11. The universal scaling function $\tilde{D}(x, 0, 1)$ of the universality class of tricritical directed percolation. For all three scaling directions (only the data within the scaling regime are plotted) the scaling plot contains at least four different curves corresponding to four different field values. The circle marks the condition $\tilde{D}(0, 0, 1) = 1$.

$$\chi(\delta p < 0, g = 0, h = 0) \sim a_{\chi,-}(-\delta p)^{-\gamma_t}, \tag{55}$$

if the critical point is approached from above and below, respectively. Using Eq. (50) the susceptibility ratio

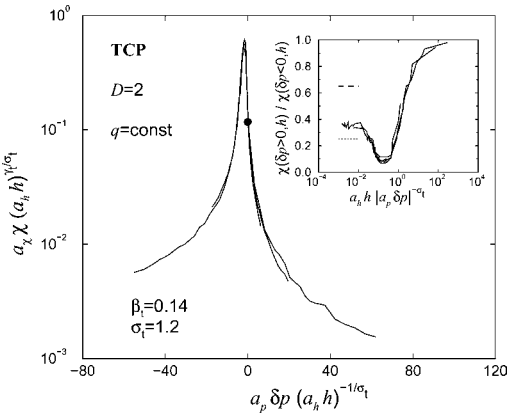

Fig. 12. The universal scaling function $\tilde{X}(x, 0, 1)$ of the universality class of tricritical directed percolation. The circle marks the condition $\tilde{X}(0, 1, 0) = \beta_t/\sigma_t$ and reflects the accuracy of the performed analysis. The inset displays the universal ratio $\tilde{X}(1, 0, x)/\tilde{X}(-1, 0, x)$. The extrapolation ($x \to 0$) yields the value of the universal amplitude ratio $\tilde{X}(1, 0, 0)/\tilde{X}(-1, 0, 0) = 0.35 \pm 0.04$. The obtained value differs significantly from the corresponding values (dashed lines) of ordinary directed percolation 0.25 for $D = 2$ and 0.65 for $D = 3$,[35] respectively.

$$\frac{\chi(\delta p > 0, 0, h)}{\chi(\delta p < 0, 0, h)} = \left.\frac{\tilde{\mathrm{X}}(a_p \delta p \lambda, 0, a_h h \lambda^{\sigma_t})}{\tilde{\mathrm{X}}(-a_p \delta p \lambda, 0, a_h h \lambda^{\sigma_t})}\right|_{a_p |\delta p| \lambda = 1}$$

$$= \frac{\tilde{\mathrm{X}}(+1, 0, x)}{\tilde{\mathrm{X}}(-1, 0, x)} \tag{56}$$

is clearly a universal quantity for all values of the scaling argument $x = a_h h |a_p \delta p|^{-\sigma_t}$. In particular it equals the ratio $a_{\chi,+}/a_{\chi,-}$ for vanishing field

$$\frac{a_{\chi,+}}{a_{\chi,-}} = \frac{\tilde{X}(+1, 0, 0)}{\tilde{X}(-1, 0, 0)}. \tag{57}$$

For example, the mean field value of the universal ratio equals 1/2.

The ratio $\tilde{\mathrm{X}}(1, 0, x)/\tilde{\mathrm{X}}(-1, 0, x)$ is shown in the inset of Fig. 12. The extrapolation to the tricritical point ($x \to 0$) yields the value of the universal amplitude ratio $\tilde{\mathrm{X}}(1, 0, 0)/\tilde{\mathrm{X}}(-1, 0, 0) = 0.35 \pm 0.05$. This value differs significantly from the corresponding values of ordinary DP for $D = 2$ and $D = 3$ (see Fig. 12 as well as Table II). Worth mentioning, the universal susceptibility ratio exhibits a non-monotonic behavior as a function of the scaling argument x. This non-monotonic behavior is a characteristic feature of TDP and does not occur in ordinary DP (see e.g. Fig. 30 of[3]).

So far simulation data are taken into account where the correlation length is small compared to the system size L. Thus, the data presented above do not suffer from finite-size effects, such as rounding and shifting of the anomalies. A typical feature of finite-size effects in equilibrium is that a given system may pass within the simulations from one phase to the other. This behavior is caused by critical fluctuations which increase if one approaches the transition point. In case of absorbing phase transitions the scenario is different. Approaching the transition point, the (spatial) correlation length $\xi_\perp$ increases. As soon as $\xi_\perp$ is of the order of L the system may pass to the absorbing state where it is trapped forever. As pointed out in[41] an appropriate way to handle that problem is to incorporate a conjugated field. Due to the conjugated field the system can not be trapped within the absorbing state and steady state quantities are available for all values of the control parameter.

As usual the system size L enters the scaling forms as an additional scaling field, e.g.

$$\rho_{\mathrm{a}} \sim \lambda^{-\beta_t} \tilde{R}(\lambda a_{\mathrm{path}} \tau_{\mathrm{path}}, 0, a_h h \lambda^{\sigma_t}, a_L L \lambda^{-\nu_{\perp,t}}) \tag{58}$$

with the tricritical exponent $\nu_{\perp,t}$ of the spatial correlation length. Using the above scaling form it is possible to determine the correlation length exponent from data of different system sizes. As well known from equilibrium, ratios of order parameter

moments $\langle \rho_a^k \rangle$ are more suited to estimate the correlation length exponent. For example, the well-known Binder cumulant $Q = 1 - \langle \rho_a^4 \rangle / 3 \langle \rho_a^2 \rangle$ was successfully investigated in numerous works (see e.g.[42]) dealing with equilibrium as well as non-equilibrium phase transitions. Furthermore, the value of the Binder cumulant at the transition point is a universal quantity.

Unfortunately, the Binder cumulant diverges at the critical point of absorbing phase transitions.[41,43] This behavior is caused by the vanishing steady state fluctuations in the absorbing phase and reflects the different nature of the zero-order parameter phase in equilibrium and in absorbing phase transitions. A ratio that remains finite at criticality is given by[43]

$$U = \frac{\langle \rho_a^2 \rangle \langle \rho_a^3 \rangle - \langle \rho_a \rangle \langle \rho_a^2 \rangle^2}{\langle \rho_a \rangle \langle \rho_a^4 \rangle - \langle \rho_a \rangle \langle \rho_a^2 \rangle^2}. \tag{59}$$

This ratio is as useful for absorbing phase transitions as the Binder cumulant Q is for equilibrium, i.e., its value at criticality characterizes the universality class. Here, we investigated the ratio U close to the tricritical point ($\tau = 0$ and $g = 0$). Its scaling behavior obeys

$$\begin{aligned} U &= \tilde{U}(\lambda \tau_{p,q}, g_{p,q} \lambda^{\phi}, h \lambda^{\sigma_t}, L \lambda^{-\nu_{\perp,t}}) \Big|_{p_t, q_t} \\ &= \tilde{U}(0, 0, h \lambda^{\sigma_t}, L \lambda^{-\nu_{\perp,t}}) \Big|_{L \lambda^{-\nu_{\perp,t}} = 1} \\ &= \tilde{U}(0, 0, h L^{\sigma_t / \nu_{\perp,t}}). \end{aligned} \tag{60}$$

The ratio U is shown in Fig. 13 for $p = 0.29931$ and $q = 0.90552$. Convincing data collapses are obtained for $\nu_{\perp,t} = 0.59 \pm 0.08$. As can be seen the ratio tends to a well defined value for $h \to 0$ independent of the system size L. The obtained value $U = 0.84 \pm 0.04$ differs significantly from the corresponding values of two-dimensional and three-dimensional ordinary DP (see Table II). Note that the determination of $U(h \to 0)$ does not depend on the critical exponents σ_t and $\nu_{\perp,t}$. But it is very sensitive to the determination of the critical point. Performing simulations slightly away from the critical point the ratio $U(h \to 0)$ displays a clear system size dependence (see inset of Fig. 13).

Thus we have determined the steady state scaling behavior of tricritical directed percolation. The obtained values of the critical exponents as well as of the universal amplitude ratios are listed in Table II. The accuracy of the estimated exponents can be checked with the scaling law

$$\gamma_t' = \nu_{\perp,t} D - 2\beta_t. \tag{61}$$

The determined two-dimensional values $\gamma_t' = 0.93 \pm 0.06$, $\nu_{\perp,t} = 0.59 \pm 0.08$, and $\beta_t = 0.14 \pm 0.02$ fulfill the above scaling law within the error bars. Furthermore, the exponent of the spatial correlation function $\eta_{\perp,t}$ is related to the

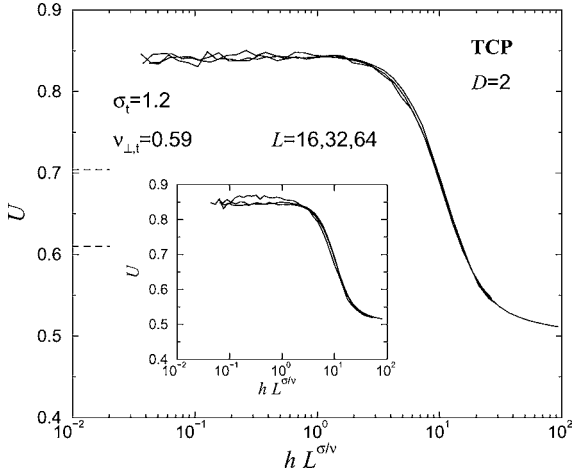

Fig. 13. Scaling plot of the ratio $U(h, L)$ close to the tricritical point ($p = 0.29931, q = 0.90552$). For vanishing field the ratio tends to the universal value $U = 0.84 \pm 0.04$ which characterizes the universality class. The dashed lines correspond to the values of $U(h \to 0)$ for two-dimensional and three-dimensional directed percolation. The inset displays the ratio slightly away from the critical point ($p = 0.29934, q = 0.90557$). The systematic deviations from a data collapse for small values of the scaling argument reflect how sensible U depends on the determination of the critical point.

correlation length exponent and to the fluctuation exponent via the Fisher scaling law

$$(2 - \eta_{\perp,\mathrm{t}})\nu_{\perp,\mathrm{t}} = \gamma_{\mathrm{t}}', \tag{62}$$

leading to $\eta_{\perp,\mathrm{t}} = 0.42 \pm 0.24$. Another quantity of interest is the fractal dimension D_{f} of growing clusters at criticality. The fractal dimension is given by[3,44]

$$D_{\mathrm{f}} = D - \frac{\beta_{\mathrm{t}}}{\nu_{\perp,\mathrm{t}}} \tag{63}$$

yielding $D_{\mathrm{f}} = 1.76 \pm 0.05$. This value is larger than the corresponding values of ordinary directed percolation ($D_{\mathrm{f},D=2} \approx 1.20$ and $D_{\mathrm{f},D=3} \approx 1.60$). A detailed investigation of the fractal behavior of critical clusters is desirable. For example, a determination of the lacunarity along the phase boundary would present a deeper understanding of the cluster propagation (see e.g.[1,45]).

It is worth comparing our numerical results to those of corresponding field theoretical analyses. Within a two-loop approach the critical exponents are given in linear order of $\epsilon = D_c - D$ by[5,22,23]

$$\beta_{\mathrm{t}} = \frac{1}{2} - \epsilon 0.4580\ldots, \tag{64}$$

$$\beta_t' = 1 + \mathcal{O}(\epsilon^2) \tag{65}$$

$$z_t = 2 + \epsilon 0.0086\ldots, \tag{66}$$

$$\nu_{\perp,t} = \frac{1}{2} + \epsilon 0.0075\ldots, \tag{67}$$

$$\gamma_t = 1 + \mathcal{O}(\epsilon^2) \tag{68}$$

$$\gamma_t' = \frac{1}{2} + \epsilon 0.4386\ldots, \tag{69}$$

$$\phi = \frac{1}{2} - \epsilon 0.0121\ldots. \tag{70}$$

Here, β' denotes the critical exponent of the survival probability. According to the ϵ-expansion one expects that the two-dimensional ($\epsilon = 1$) values of the exponents $\nu_{\perp,t}$, γ_t, and ϕ differ only slightly from their mean field values. Whereas strong deviations are predicted by the ϵ-expansion for β_t and γ_t'. This behavior is confirmed by our numerical results. But one has to mention that the field theorically estimated exponents differ significantly from the numerical values. For example, the ϵ-expansion yields for the order parameter exponent $\beta_t = 0.042\ldots$. This value differs by 70% from the numerical value. Furthermore, the RG results predict $\phi < 1/2$ whereas the simulations clearly show $\phi > 1/2$. Thus an ϵ-expansion of higher-orders than $\mathcal{O}(\epsilon)$ is desirable to describe the scaling behavior by a field theoretical approach.

6. FIRST-ORDER PHASE TRANSITION

In this section we investigate the first-order regime of the modified contact process. A general phenomenon associated with first-order transitions is the presence of hysteresis by cycling across the transition. In equilibrium, the hysteresis is related to the effects of supercooling and superheating. Analogous effects occur in case of the modified contact process. First we investigate the effect of superheating, i.e., we consider the order parameter within the active phase ($\rho_a > 0$) while approaching the transition point (on heating in equilibrium). Decreasing the parameter p for fixed $q > q_t$ the order parameter jumps at a certain point p_o from a finite value to zero. This is shown in Fig. 14 for $q = 0.97$. Close to $p_o = 0.221$ the order parameter behaves discontinuously. This transition point p_o corresponds to the limit of superheating. Note that in contrast to a continuous phase transition the transition point p_o exhibits no systematic system size dependence.

The similar phenomenon of supercooling the zero-order parameter phase is usually not accessible for absorbing phase transitions. Owing to the lack of fluctuations for $\rho_a = 0$ the system can never escape the absorbing state by a variation of p and q, respectively. To avoid that the system is trapped within the

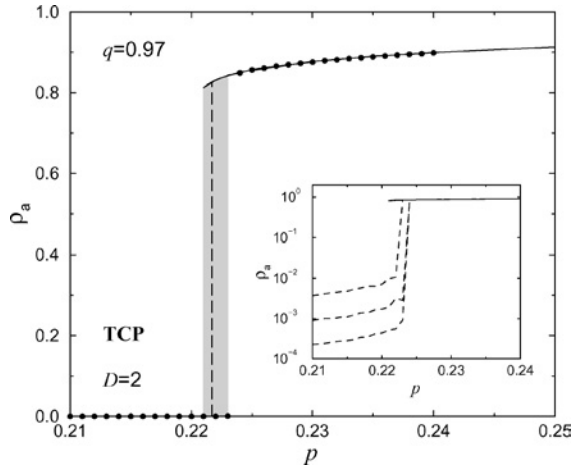

Fig. 14. The order parameter behavior within the first-order regime of the tricritical contact process (TCP). The solid line is obtained from steady state measurements at zero field for various system sizes. Within the simulations the control parameter p is slowly decreased until the absorbing state is reached. The circles correspond to data which are obtained from finite-field simulations and slowly increasing parameter p. Within the shadowed area the active and the absorbing phase coexist. The dashed line marks the transition point p_c obtained from a stability analysis of separated phases (see text). The inset shows the field dependence of the order parameter (for growing p). The three dashed lines correspond to three different field values (from $h = 410^{-4}$ (top) to $h = 310^{-5}$). As can be seen, a well defined upper limit of the supercooled low density phase can be obtained.

absorbing state an external field h is applied. In that way it is possible to perform steady state measurements of the order parameter on cooling, i.e., within in the low density phase ($\rho_a \ll 1$) for increasing p. The resulting curves are shown in the inset of Fig. 14. At a certain value $p_u(h)$ the order parameter jumps from a low density value to a high density value. Note that the low density value of ρ_a tends to zero for vanishing field. Furthermore, a well defined transition value $p_u(h)$ exists for $h \to 0$. The obtained value $p_u \approx 0.223$ corresponds to the limit of supercooling.

In that way we have obtained from steady state measurements a small but finite hysteresis, i.e., the two phases coexist between $p_o < p < p_u$. Within the active phase ($\rho_a \approx 0.8$) the system is stable against small fluctuations until p_o is reached from above. On the other hand the absorbing phase is stable against external fluctuations, triggered by the conjugated field, until p_u is approached from below. Snapshots of the system within the supercooled and superheated state are shown in Fig. 15.

Finally we address the question of the critical value $p_c(q)$ of the first-order phase transitions. In equilibrium, the transition point is related to a thermodynamical potential such as the free energy. At the critical temperature the free energy

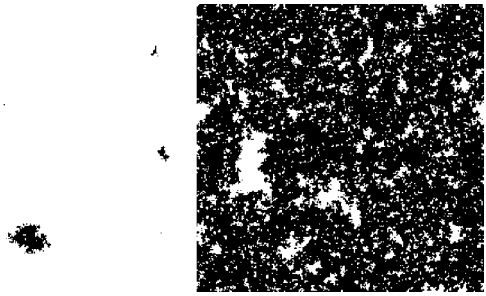

Fig. 15. Snapshots of the tricritical contact process within the regime of first-order phase transitions ($q = 0.97$ and $L = 256$). The left figure shows a typical low density configuration ($p = 0.223$, supercooled phase). The seeds are triggered by an external field $h = 10^{-4}$. The right figure displays a high density configuration ($p = 0.221$, superheated phase). Here, order parameter fluctuations lead to seeds of various sizes. In both cases the seeds are subcritical, i.e., they disappear after a certain lifetime.

of both phases are equal. Unfortunately, this definition can not be applied to the considered non-equilibrium phase transition. An alternative way of defining the first-order transition point is based on the behavior of moving interfaces which separate both phases. In case of phase equilibrium the interface velocity is zero whereas it is non-zero if one phase is favored by the dynamics.

According to that picture we have investigated the phase propagation within the first-order regime. Initially the system contains a stripe (width $L/2$) of occupied particles. All lattice site outside the stripe remains empty. Depending on p and q, the system reaches after a transient either the absorbing phase or a steady state of a homogeneous non-zero particle density. Snapshots are shown in Fig. 16. For $q = 0.97$ and $L = 256$ we have performed more than 50 runs for each value of p. The dynamics are attracted by the empty lattice in all runs for $p \leq 0.2215$. On the other hand the active phase is always approached for $p \geq 0.2219$. For $p = 0.2217$ both phases appear with probability of roughly 1/2. Thus an interval exists where both phases are favored by the dynamics. But we observe that this interval decreases with increasing system size L, i.e., a well defined transition point $p_c(q)$ exists in the thermodynamic limit. For $q = 0.97$ the value $p_c = 0.2217$ is obtained (see Fig. 14) yielding an asymmetric hysteresis between $0.221 < p < 0.223$.

The above analysis of the first-order transition is performed for a fixed value of q. Varying q the first-order transition line $p_c(q)$ as well as the borderlines of supercooling $p_u(q)$ and superheating $p_o(q)$ can be determined. In order to limit the numerical effort we focus to the determination of p_o. Since the hysteresis is quite narrow ($\Delta p/p_c \approx 0.009$) p_u presents a sufficient approximation of the transition line. The corresponding values are plotted in Fig. 7. Remarkably, the first-order line ends for $q \to 1$ at a finite p value in contrast to the mean field phase diagram (see Fig. 1).

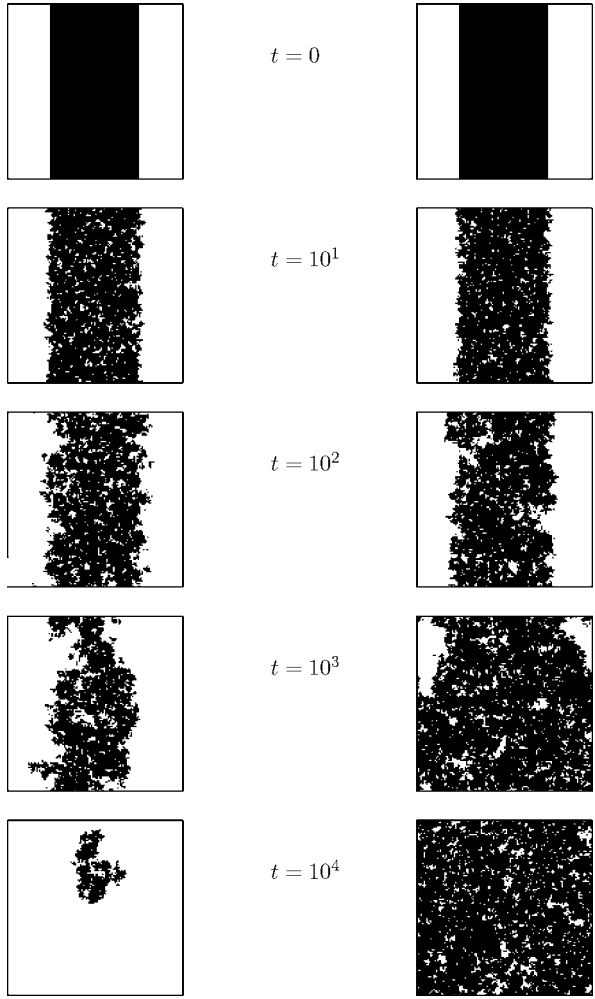

Fig. 16. Snapshots of the tricritical contact process close to the first-order transition for $q = 0.97$ and $L = 128$ (periodic boundary conditions are applied). Starting from a stripe of particles the dynamics is attracted either by the empty lattice (left, $p = 0.22$, the eventual occurring empty lattice is not shown) or by a steady state of a homogeneous non-zero particle density (right, $p = 0.24$). The time t is measured as the number of lattice updates.

7. CONCLUSION

In summary, we have considered a modification of the well established contact process in order to study the process of tricritical directed percolation. Taking pair reactions into account the modified process exhibits a non-trivial phase diagram

containing a tricritical point. The tricritical point separates a line of second-order phase transitions from a line of first-order phase transitions. The transition along the second-order line belong to the universality class of directed percolation. Performing a simple scaling analysis the tricritical point is determined with high accuracy. This allows a detailed analysis of the tricritical scaling behavior within the steady state. In particular, we have determined the tricritical exponents, universal scaling functions as well as universal amplitude ratios. The obtained values of the critical exponents as well as the universal amplitude ratios are listed in Table II. Additionally we have investigated the first-order regime. A hysteresis is found from steady state measurements. Owing to effects of metastability supercooling and superheating phenomena are observed. An analysis of the dynamical scaling properties of tricritical directed percolation will be published elsewhere.

ACKNOWLEDGMENTS

I would like to thank H.-K. Janssen, A. Hucht, G. ÓAdor, and P. Grassberger for fruitful discussions.

REFERENCES

1. H. Hinrichsen. *Adv. Phys.* **49**:815 (2000).
2. G. Ódor. *Rev. Mod. Phys.* **76**:663 (2004).
3. S. Lübeck. *Int. J. Mod. Phys. B* **18**:3977 (2004).
4. J. Marro and R. Dickman, *Nonequilibrium phase transitions in lattice models* (Cambridge University Press, Cambridge, 1999).
5. H.-K. Janssen. *J. Phys.: Cond. Mat.* **17**:S1973 (2005).
6. H.-K. Janssen. *Z. Phys. B* **42**:151 (1981).
7. P. Grassberger. *Z. Phys. B* **47**:365 (1982).
8. S. Lübeck and R. D. Willmann. *Nucl. Phys. B* **718**:341 (2005).
9. H.-K. Janssen. *Phys. Rev. E* **55**:6253 (1997).
10. I. Jensen. *Phys. Rev. Lett.* **77**:4988 (1996).
11. A. G. Moreira. *Phys. Rev. E* **54**:3090 (1996).
12. R. Cafiero, A. Gabrielli, and M. A. Muoz. *Phys. Rev. E* **57**:5060 (1998).
13. J. Hooyberghs, F. Iglói, and C. Vanderzande. *Phys. Rev. E* **69**:066140 (2004).
14. T. Vojta and M. Dickison. *Phys. Rev. E* **72**:036126 (2005).
15. E. Domany and W. Kinzel. *Phys. Rev. Lett.* **53**:311 (1984).
16. J. W. Essam. *J. Phys. A* **22**:4927 (1989).
17. S. S. Manna, *J. Phys. A* **24**:L363 (1991).
18. M. Rossi. R. Pastor-Satorras, and A. Vespignani, *Phys. Rev. Lett.* **85**:1803 (2000).
19. S. Lübeck and P. C. Heger. *Phys. Rev. Lett.* **90**:230601 (2003).
20. D. Zhong and D. ben Avraham. *Phys. Lett. A* **209**:333 (1995).
21. J. L. Cardy and U. C. Täuber. *Phys. Rev. Lett.* **13**:4780 (1996).
22. T. Ohtsuki and T. Keyes. *Phys. Rev. A* **35**:2697 (1987).
23. T. Ohtsuki and T. Keyes. *Phys. Rev. A* **36**:4434 (1987).
24. H.-K. Janssen, M. Müller, and O. Stenull. *Phys. Rev. E* **70**:026114 (2004).
25. A. P. Atman, R. Dickman, and J. G. Moreira. *Phys. Rev. E* **67**:016107 (2003).

26. K. E. Bassler and D. A. Browne. *Phys. Rev. Lett.* **77**:4094 (1996).
27. F. Bagnoli, N. Boccara, and R. Rechtman. *Phys. Rev. E* **63**:046116 (2001).
28. T. E. Harris. *Ann. Prob.* **2**:969 (1974).
29. G. Ódor, private communication (2005).
30. R. Dickman and T. Ťomé. *Phys. Rev. A* **44**:4833 (1991).
31. R. M. Ziff and B. J. Brosilow. *Phys. Rev. A* **46**:4630 (1992).
32. B. J. Brosilow and R. M. Ziff. *Phys. Rev. A* **46**:4534 (1992).
33. S. Lübeck and R. D. Willmann. *J. Phys. A* **35**:10205 (2002).
34. H. Mori and K. J. McNeil. *Prog. Theor. Phys.* **57**:770 (1977).
35. S. Lübeck and R. D. Willmann. *J. Stat. Phys* **115**:1231 (2004).
36. J. L. Cardy and R. L. Sugar. *J. Phys. A* **13**:L423 (1980).
37. S. P. Obukhov. *Physica A* **101**:145 (1980).
38. T. M. Liggett. *Interacting particle systems* (Springer, New York, 1985).
39. R. Dickman. *Phys. Rev. E* **60**:2441 (1999).
40. E. Luijten, H. W. J. Blöte, and K. Binder. *Phys. Rev. Lett.* **79**:561 (1997).
41. S. Lübeck and P. C. Heger. *Phys. Rev. E* **68**:056102 (2003).
42. K. Binder and D. W. Heermann, *Monte Carlo Simulation in Statistical Physics* (Springer, Berlin, 1997).
43. S. Lübeck and H.-K. Janssen. *Phys. Rev. E* **72**:016119 (2005).
44. P. Grassberger. *J. Phys. A* **22**:3673 (1989).
45. J. C. Lee. *J. Phys. A* **24**:L377 (1991).
46. C. A. Voigt and R. M. Ziff. *Phys. Rev. E* **56**:R6241 (1997).
47. P. Grassberger and Y.-C. Zhang. *Physica A* **224**:169 (1996).
48. I. Jensen. *Phys. Rev. A* **45**:R563 (1992).